# Acquired resistance with epigenetic alterations under long-term anti-angiogenic therapy for hepatocellular carcinoma

Yoshiteru Ohata[1,2], Shu Shimada[1], Yoshimitsu Akiyama[1], Kaoru Mogushi[1], Keisuke Nakao[2], Satoshi Matsumura[2], Arihiro Aihara[2], Yusuke Mitsunori[2], Daisuke Ban[2], Takanori Ochiai[2], Atsushi Kudo[2], Shigeki Arii[2], Minoru Tanabe[2], and Shinji Tanaka[1,2]

[1]Department of Molecular Oncology, Graduate School of Medicine, Tokyo Medical and Dental University, Tokyo, Japan. [2]Department of Hepato-Biliary-Pancreatic Surgery, Graduate School of Medicine, Tokyo Medical and Dental University, Tokyo, Japan.

**Running title:** Resistance to anti-angiogenic therapy with epigenetic change

**Keywords:** Liver cancer; Angiogenesis inhibitors; Drug resistance; Epigenetic alteration; Stemness; Thymosin β 4.

**Grant support:** This work was supported by Grant-in-Aid for Scientific Research (A), Scientific Research on Innovative Areas, Challenging Exploratory Research from the

Ministry of Education, Culture, Sports, Science and Technology of Japan; Research Grant from the Princess Takamatsu Cancer Research Fund; P-DIRECT, P-CREATE, and Research Program on Hepatitis from AMED (Japan Agency for Medical Research and Development).

**Corresponding Author:** Shinji Tanaka, Department of Molecular Oncology, Tokyo Medical and Dental University, 1-5-45 Yushima, Bunkyo-ku, Tokyo 113-8519, Japan. Phone: 81-3-5803-5182; Fax: 81-3-5803-0125; E-mail: tanaka.monc@tmd.ac.jp

**Disclosure of Potential Conflicts of Interest:** No potential conflicts of interest were disclosed by the authors.

**Word count:** 5497

**Total number of figures and tables:** 6

**Abstract**

Anti-angiogenic therapy is initially effective for several solid tumors including hepatocellular carcinoma (HCC); however, they finally relapse and progress, resulting in poor prognosis. We here established in vivo drug-tolerant subclones of human HCC cells by long-term treatment with vascular endothelial growth factor receptor (VEGFR) inhibitor and serial transplantation in immunocompromised mice (total 12 months), and then compared them with the parental cells in molecular and biological features. Gene expression profiles elucidated a G-actin monomer binding protein thymosin β 4 (Tβ4) as one of the genes enriched in the resistant cancer cells relative to the initially sensitive ones. Highlighting epigenetic alterations involved in drug resistance, we revealed that Tβ4 could be aberrantly expressed following demethylation of DNA and active modification of histone H3 at the promoter region. Ectopic overexpression of Tβ4 in HCC cells could significantly enhance sphere-forming capacities and infiltrating phenotypes in vitro, and promote growth of tumors refractory to the VEGFR mutltikinase inhibitor sorafenib in vivo. Clinically, sorafenib failed to improve the progression-free survival in patients with Tβ4-high HCC, indicating that Tβ4 expression could be available as a surrogate marker of susceptibility to this drug. This study suggests that Tβ4 expression triggered by epigenetic alterations could contribute to the

development of resistance to anti-angiogenic therapy by the acquisition of stemness, and that epigenetic control might be one of the key targets to regulate the resistance in HCC.

## Introduction

Hepatocellular carcinoma (HCC) is the second most frequent cause of cancer-related mortality worldwide (1, 2). Since the SHARP and Asian-Pacific trials successfully demonstrated that sorafenib prolonged overall survival in patients with advanced HCC, it has become the standard of care in this setting (3). A phase I/II trial of lenvatinib for HCC patients in Child-Pugh class A recently reported that 14 of 46 patients enrolled have partial response, and a phase III trial was designed to compare the efficacy of lenvatinib and sorafenib (4). In the randomized, double-blind, placebo-controlled international phase III trial (RESORCE), regorafenib achieved an overall survival improvement in patients with HCC progressing on sorafenib treatment (5). All the three drugs are classified as multikinase inhibitors mainly targeting angiogenesis through vascular endothelial growth factor receptor (VEGFR). We previously reported that a novel VEGFR and aurora kinase inhibitor JNJ-28841072 remarkably suppresses tumor growth of human HCC cell lines by decreasing neovascularization (6), suggesting the angiogenesis-dependency as an essential hallmark of HCC.

Although the introduction of anti-angiogenic therapy leads to tumor regression and in some cases extended survival, the tumors inevitably progress again after a short

term of clinical benefit (7). In the phase III C-08 trial of adjuvant therapy prior to surgery for colorectal cancer, the addition of a humanized anti-VEGF monoclonal antibody bevacizumab transiently improved disease-free survival during the initial year of treatment but not during the remaining period (8). In xenograft mouse models, the tumors showed transient response to VEGFR antagonists, but became more aggressive, invasive and metastatic following several weeks of administration (9). There is a clear need to reveal the mechanistic basis of this apparent conundrum for the therapeutic targeting of tumor angiogenesis.

Several laboratories have mentioned that epigenetic events are implicated in drug resistance in tumor cells treated with targeted agents such as hormone therapy and tyrosine kinase inhibitors (10-15). Tamoxifen- and fulvestrant-resistant sublines of MCF7 breast cancer cells have diverse gene expression and DNA methylation profiles (12). H3K4 methylation states were altered by the elevated expression of histone demethylase RBP2/KDM5A/JARID1A in gefinitib-tolerant PC9 non-small cell lung cancer cells (13). However, the epigenetic mechanisms underlying drug resistance to anti-angiogenic therapy are poorly understood.

Therefore, we derived in vivo drug-tolerant HCC cells by repeated treatment of VEGFR inhibitor and serial transplantation in immunodeficient mice for 12 months and

identified that aberrant expression of thymosin β 4 (Tβ4) caused by epigenetic alterations could contribute to the achievement of resistance (16).

## Materials and Methods

### Cell culture, animal studies, and chemical drugs

The human HCC cell line HuH7 was obtained from the Human Science Research Resources Bank (Osaka, Japan), authenticated by short tandem repeat DNA fingerprinting (BEX Co. Ltd., Tokyo, Japan). It was cultured in RPMI 1640 (Wako, Osaka, Japan) supplemented with 10% fetal bovine serum, 100 U/ml penicillin, and 100 μg/ml streptomycin (Invitrogen, Carlsbad, CA), maintained in a humidified incubator at 37°C in 5% CO2, and harvested with 0.05% trypsin-0.03% EDTA (Invitrogen). NOD/SCID (NOD.CB17-*Prkdc*$^{scid}$/J) mice were purchased from Charles River Laboratories (Wilmington, MA). All mouse procedures were approved by the Institutional Animal Care and Use Committee of our institute (permission No. 0160074A). JNJ-28841072 (7-[1H-indol-2-yl]-2, 3-dihydro-isoindol-1-ones) was generously provided by Janssen Pharmaceutical Research and Development (Spring House, PA), and sorafenib tosylate was purchased from Selleck (Houston, TX).

**Clinical samples**

Three hundred and eight patients underwent curative hepatectomy for HCC from 2009 and 2014 at Tokyo Medical and Dental University Hospital. Among them, 30 patients were postoperatively treated with sorafenib (400-800mg/day) for the recurrence. The initially resected tissues were fixed in 10% formaldehyde solution and embedded in paraffin for histopathological analysis. Written informed consent was received from all the patients in this study with the approval of Institutional Review Board of our institute (permission No. 1080).

**Serial transplantation and repeated treatment**

Tumors derived from HuH7 were roughly minced into small pieces and immediately transplanted into NOD/SCID mice. When the tumors reached 100 to 150 $mm^3$ in volume, JNJ-28841072 (100 mg/kg/day) was intraperitoneally administered into the mouse on two consecutive days per week for two weeks, but tumors composed of resistant cancer cells developed up to day 28. This procedure was repeated up to 12 times, and cancer cells established from the 6th and 12th generation of the resistant tumors served as HuH7-F6 and -F12, respectively.

**Tumor seeding and drug administration**

Cells were suspended in 100 μl Matrigel (BD Biosciences, San Jose, CA) and subcutaneously injected into NOD/SCID mice. The volume of the growing tumors was monitored every two days, and calculated by the formula; volume = length × width$^2$ × 0.5. JNJ-28841072 (100 mg/kg/day) and sorafenib (30 mg/kg/day) were administered after tumors became palpable (approximately 250 mm$^3$).

**RNA extraction and microarray analysis**

Total RNA was extracted from cells by using RNeasy Protect Mini Kit (QIAGEN, Hilden, Germany). The integrity of the obtained RNA was confirmed by using 2100 Bioanalyzer (Agilent Technologies, Santa Clara, CA). Contaminating DNA was removed by digestion with RNase-Free DNase Set (QIAGEN). Complementary RNA was prepared from 100 ng of total RNA from each sample with 3' IVT Express Kit (Affymetrix, Santa Clara, CA). The hybridization and signal detection of GeneChip Human Genome U133 Plus 2.0 Array (Affymetrix) were performed in accordance with the manufacturer's instructions. Gene expression data have been deposited in the Gene Expression Omnibus (GEO) under accession GSEGSE93595.

**Bioinformatics**

The four microarray datasets of two pairs of the parental (HuH7-F0) and filial HCC cell lines (HuH7-F6 and -F12) were normalized by using the robust multiarray average method in the R statistical software (version 3.0.3) and the Affy Bioconductor package. To investigate how the biological functions changed during the acquisition of resistance to anti-angiogenic therapy, the gene set enrichment analysis (GSEA) was performed with the MSigDB gene sets (C2: chemical and genetic perturbations; version 5.0).

**Quantitative RT-PCR**

For single-stranded complementary DNA synthesis, 1 μg of total RNA was reverse-transcribed by SuperScript III Reverse Transcriptase (Invitrogen). The primer sets and amplification conditions for polymerase chain reaction (PCR) are listed in Supplementary Table S1. Glyceraldehyde-3-phosphate dehydrogenase RNA was used as an endogenous control.

**Methylation analysis**

Genomic DNA was obtained from cells by phenol-chloroform extraction.

Bisulfite treatment of DNA was performed with EZ DNA Methylation-Gold (Zymo Research, Irvine, CA), and then methylation-specific PCR (MSP) and bisulfite sequencing (BSS) were conducted. Briefly, the PCR reaction was performed for 35 cycles in a 25 μl mixture comprising bisulfite-modified DNA, 2.5μl of 10× PCR buffer, 1.25 μl of 25mM dNTPs, 25 pmol/l of each primer, and 1 U of JumpStart RedTaq polymerase (Sigma-Aldrich, St. Louis, MO). The conditions for PCR were listed in Supplementary Table S1.

**Histone modification analysis**

Chromatin immunoprecipitation (ChIP) assay was performed by using ChIP-IT Express Kit (Active Motif, Carlsbad, CA) according to the manufacturer's protocol. Immunoprecipitated DNA enrichment was normalized as to the input. The antibodies used in this study were anti-H3K4me3, anti-H3K9me3, anti-H3K27me3, and anti-H3K27ac, all of which were purchased from Active Motif. Normal rabbit IgG (Cell Signaling Technology, Danvers, MA) was used as a negative control for each assay.

**Western blotting**

Cells were lysed by using RIPA Buffer (Thermo Fisher Scientific, Waltham,

MA) with a protease inhibitor cocktail kit (Sigma Aldrich, St. Louis, MO). Aliquots containing 30 μg of cell lysates were denatured in 5× Sample Buffer (Wako), electrophoretically resolved on SDS-polyacrylamide gels (Wako), and then transferred onto Immobilon polyvinyldifluoride membranes (Millipore, Billerica, MA). The membrane blots were blocked with 2% skimmed milk (Cell Signaling Technology) for an hour at room temperature, and then incubated with primary antibodies at 4 °C overnight. After the appropriate secondary antibodies were added for an hour, the signals were developed with Immun-Star AP Substrate (Bio-Rad, Hercules, CA) and observed by using LAS-3000 (Fujifilm, Tokyo, Japan).

**Overexpression of Tβ4**

The Tβ4 construct was amplified by using the primer pair shown in Supplementary Table S1, and subcloned into HindIII and BamHI sites in pEGFP-N1 (Clontech Laboratories, Mountain View, CA). HuH7 cells were transfected with the plasmid for Tβ4-EGFP fusion protein expression by using Neon Transfection System (Invitrogen). The transfected cells were selected in culture media containing 400 μg/ml G418 (Invitrogen), and utilized as HuH7-Tβ4 cells in this study.

**Immunocytochemistory**

Cells were seeded onto small coverslips in 6-well plates, and incubated for 24 hours to allow cell attachment. The cells were fixed with 4% paraformaldehyde at 4 °C for 15 minutes, and permeabilized with 0.1% Triton X-100 for five minutes prior to incubation in 3% bovine serum albumin for 30 minutes at room temperature. The blocking buffer was removed and the cells were incubated with primary antibodies at 4 °C for an hour. After washing with phosphate buffered saline, they were additionally incubated with fluorescence-conjugated secondary antibodies (Invitrogen) for an hour, and the cellular DNA was subsequently covered and labelled with ProLong Gold antifade reagent with DAPI (Invitrogen). The slides were viewed with a fluorescent microscope (Carl Zeiss, Oberkochen, Germany).

**Sphere-forming assay**

HuH7-F0, -F12 and -Tβ4 cells were plated separately at several densities from 1000 to 2000 cells in low attachment plates (24-well Ultra Low Cluster Plate; Corning, Corning, NY), and incubated in serum-free Dulbecco's modified Eagle medium/F12 media (Wako), and the total number of spheres was counted a week after incubation.

**Migration and invasion assay**

The double-chamber migration assay was performed by using a transwell chamber (24-well plate, 8-μm pores; BD Biosciences). For the invasion assay, matrigel-coated (BD Biosciences) transwells (0.1 mg/ml) were prepared by incubation in serum-free media for two hours at 37°C in 24-well plates. The lower chambers were filled with 0.8 ml culture media without antibiotics. Then, cancer cells ($8 \times 10^4$ in 0.3 ml serum-free media) were seeded onto the upper chambers and incubated at 37°C for 24 hours. The cells on the upper surface of the filters were removed by using cotton wool swabs. The remaining cells were then fixed with 100% methanol and stained with Giemsa solution, and the number of cells migrating or infiltrating into the lower surface was counted in three randomly selected high-magnification fields (100×) for each sample.

**Immunohistochemistory**

Transplanted tumor tissues were fixed overnight in 4% paraformaldehyde, embedded in paraffin, and sectioned (4 μm thick). Tumor specimens of the 30 HCC patients described above were also sectioned (4 μm thick). They were stained with an automated immunostainer (DISCOVERY XT; Ventana Medical Systems, Tucson, AZ)

by using heat-induced epitope retrieval and a standard diaminobenzidine detection kit. Incubation times for the primary and secondary antibodies were 2 and 1 hour, respectively. The primary antibodies used were anti-Tβ4 (sc-67114, 1:200; Santa Cruz Biotechnology, Dallas, TX) and anti-CD31 (ab28364, 1:50; Abcam, Cambridge, UK). Secondary antibodies included universal secondary antibody (Ventana Medical Systems). All tissue sections were counterstained with hematoxylin.

**Statistical analysis**

Statistical analysis was performed by using SPSS statistics Version 23.0 (IBM, Armonk, NY). Two-sided Student's *t* tests and multiple comparison tests were used to analyze for differences between continuous values of two independent groups. The Fisher's exact test was applied to analyze categorical variables. Survival curves were constructed by using the Kaplan-Meier method and compared with the log-rank test. *P*-value less than 0.05 was considered statistically significant.

**Results**

**Generation of hepatocellular carcinoma cells with in vivo resistance to anti-angiogenic drugs**

To clarify the mechanism of in vivo resistance to long-term anti-angiogenic therapy in HCC, we first established a xenograft mouse model as schematically represented in Fig. 1A. Briefly, after the VEGFR and aurora kinase inhibitor JNJ-28841072 was intraperitoneally injected into NOD/SCID mice bearing tumors of HuH7 cells, the tumors eliciting resistance to this inhibitor were excised into small aliquots and directly engrafted in a second group of NOD/SCID mice. By repeating this process 6 and 12 times, drug-refractory HuH7-F6 and -F12 cells were derived from the parental cancer cells (HuH7-F0), respectively. We validated that JNJ-28841072 reduced the size of transplanted tumors of HuH7-F0, but not those of HuH7-F12 (Fig. 1B). Sorafenib, an anti-angiogenic drug approved for advanced HCC, could not extend survival time in the mice with HuH7-F6 or -F12 tumors because of failure to suppress the tumor growth (Fig. 1C and D). Thus, HuH7-F6 and -F12 exhibited enhanced in vivo tolerance to anti-angiogenic therapy.

**Identification of genes associated with anti-angiogenic drug resistance**

Microarray analysis was performed to compare gene expression patterns between HuH7-F0, -F6 and -F12. The GSEA demonstrated that gene signatures involved in stem cell features; *embryonic, neural & hematopoietic stem cell-like* (17)

and *hepatoblastoma-like* (18), as well as proliferative phenotypes; *subclass S2 of Hoshida's classification* (19) and *subclass G2 of Boyault's classification* (20) were extremely augmented in the two resistant cancer cells (Fig. 2A), consistent with the recent findings that sorafenib-resistant HCC xenografts exhibit the similar molecular characteristics (21). Next, the expression levels of 119 genes were more than four-fold upregulated in HuH7-F6 cells while those of 2199 genes in HuH7-F12 (Fig. 2B). Among the genes differentially expressed between the acquired resistant and sensitive cancer cells (Supplementary Table S2), we highlighted thymosin β 4, X-linked (Tβ4), which is a G-actin monomer binding protein involved in actin-cytoskeleton organization. In the microarray data, Tβ4 was one of the most overexpressed genes in both HuH7-F6 and -F12 (27.7- and 30.7-fold in the microarray data as shown in Supplementary Table S2), which was confirmed by quantitative PCR (Fig. 2C). We also found that the expression level of CD133, a liver progenitor marker, was upregulated in these two sublines (Fig. 2C).

**Correlation between DNA methylation at the Tβ4 promoter region and its gene expression**

Several previous findings have implicated a distinct epigenetic status in the maintenance of drug resistance (10-15). To determine the transcriptional regulation of Tβ4 by epigenetic mechanism, we initially exposed HuH7 cells to two epigenetic drugs, a demethylating agent 5-aza-2'-deoxycytidine (5-aza-dC) and a histone deacetylase (HDAC) inhibitor trichostatin A (TSA). The Tβ4 expression levels were markedly elevated not only in the cells treated with 5-aza-dC treatment but also cells treated with TSA (Fig. 3A), implying that epigenetic changes could be important to Tβ4 expression in HuH7 cells.

Since the human Tβ4 gene contains an extensive CpG island from the promoter region to the exon 2 according to the UCSC database and the Methprimer program (Fig. 3B), we investigated methylation states at the promoter in each HuH7 subclone. In MSP, HuH7-F0 cells harbored dense methylation at the region (Fig. 3C), and the PCR band displayed unmethylated DNA in HuH7-F0 cells with 5-aza-dC treatment (data not shown). On the other hand, both methylated and unmethylated patterns were detected at the same locus in HuH7-F6 and -F12 cells (Fig. 3C). Bisulfite sequencing illustrated that the methylation ratio of HuH7-F0, -F6 and -F12 were 94.0%, 55.8% and 45.3%, respectively (Fig. 3D). These findings indicated demethylation at the Tβ4 promoter during the formation of sorafenib resistance.

**Histone modification involved in Tβ4 expression**

Since histone modification may be associated with Tβ4 expression as well as DNA methylation (Fig. 3A), we examined the methylation status of histone H3, that is, the levels of H3K4 trimethylation (me3), H3K9me3, and H3K27me3 in HuH7-F0 and its clonal cells by using semi-quantitative ChIP assay. Among the three regions (CP1, CP2 and CP3) of the Tβ4 gene (Fig. 4A), the levels of H3K4me3 at the CP2 region in HuH7-12 cells were higher than those in HuH7-F0 (Fig. 4B), but the H3K9me3 and H3K27me3 levels at the three regions were not distinct between the two cell lines. The patterns of the H3K27ac levels, which are known to be restored by inhibiting HDAC activity, were very similar to those of the H3K4me3 (Fig. 4B). Quantitative ChIP analysis demonstrated that the H3K4me3 and H3K27 acetylation (ac) levels at the CP2 region in HuH6-F6 and -F12 cells were significantly increased compared with those in HuH7-F0 cells (Fig. 4C). Thus, active marks of histone modification, H3K4me3 and H3K27ac, were enriched at the promoter region in the drug-refractory subclones with high Tβ4 expression. Additionally, the protein levels of H3K4me3 and H3K27ac were more strongly upregulated in HuH-F6 and -F12 than those in HuH7-F0 (Fig. 4D), implying genome-wide alterations of histone modification.

**Acquisition of cancer stem cell-like abilities by increased expression of Tβ4**

To investigate the oncogenic role of Tβ4 in HCC cells, we employed a gain-of-function strategy by using HuH7 cells stably overexpressing Tβ4 (HuH7-Tβ4), which was observed by immunocytochemistry (Fig. 5A). Considering the enrichment of stem cell properties and aggressive phenotypes in the subclones of HuH7 cells refractory to anti-angiogenic therapy (Fig. 2A), we characterized biological traits of HuH7-F12 and -Tβ4 in vitro. HuH7-Tβ4 cells strikingly generated spheres at higher frequency than HuH7-F0, similarly to HuH7-F12 (Fig. 5B) (21). Compared with HuH7-F0, HuH7-F12 and -Tβ4 showed increased cellular migration and invasion capacities (Fig. 5C and D).

Overexpression of Tβ4 promoted tumor growth in vivo (Fig. 6A), which was immunohistochemically validated in the xenograft of HuH7-F12 and -Tβ4 (Fig. 6B). We next evaluated the in vivo effects of Tβ4 on resistance to anti-angiogenic therapy. Similarly to the sorafenib-resistant F12, HuH7-Tβ4 tumors were refractory to the VEGFR inhibitor, resulting in short survival periods and large tumor volumes (Fig. 6C and D). Sorafenib targeting VEGF pathway could exhibit anti-angiogenic activity in the HuH7-F0 tumors, but not in the HuH7-F12 or -Tβ4 tumors (Fig. 6E and 6F). Taken

together, ectopic expression of Tβ4 in HCC cells could mimic malignant transformation undergone in the course of acquired resistance to anti-angiogenic drugs.

**Clinical significance of Tβ4 expression in HCC patients treated with sorafenib**

The clinicopathological significance of Tβ4 expression was surveyed in 30 patients receiving sorafenib administration in our institute (22). Seven HCC samples displayed strong positive staining for Tβ4, whereas 23 did weak or no staining (Fig. 7A), and there was no difference in any clinical factors between the Tβ4-high and -low groups (Supplementary Table S3). It is noteworthy that the progression-free survival time of the Tβ4-high was markedly shortened compared with that of the Tβ4-low/negative group (Fig. 7B), suggesting that Tβ4 expression could predict the prognosis of patients treated with anti-angiogenic therapy.

**Discussion**

We elucidated the mechanism underlying acquired resistance to anti-angiogenic therapy by using a xenograft mouse model in this research. While the study of in vivo effects was necessarily more difficult than in vitro, an understanding of the factors may be critical to the development of strategies to overcome or prevent the emergence of

drug tolerance (16). Moreover, since sorafenib and other kinase inhibitors approved for HCC mainly target the tumor microenvironment by deregulating VEGF-dependent angiogenesis, only in vivo models recapitulate the process of acquired resistance in the clinic. Two groups have elegantly demonstrated sorafenib resistance in HCC by using in vivo models. Rudalska et al. performed screening assays with hydrodynamic tail-vein injection of $Nras^{G12V}$ and a focused shRNA library into $p19^{Arf}$-deficient mice, and then identified that silencing of Mapk14 could sensitize mouse HCC to sorafenib therapy (23). Establishing HCC xenograft mouse models treated with a cycle of sorafenib, Tovar et al. compared the biological and molecular properties between resistant and sensitive tumors, and argued that acquisition of tumor-initiating cell-like features and activation of IGF/FGF signaling could cause drug tolerance (12). We here presented a potent strategy of repeated administration, which is more closely similar to therapeutic use for HCC than the two prior studies.

Molecular analysis extracted Tβ4 as a gene overexpressed in the HCC subclone cells refractory to multiple VEGFR inhibitors (Fig. 2), and the clinical expression of Tβ4 could predict the prognosis of HCC patients treated with sorafenib (Fig. 7). Several previous studies have hinted that Tβ4 might contribute to the development of resistance to these types of anti-cancer drugs; Tβ4 overexpression accelerated malignant

progression including tumor xenograft growth in colorectal cancer cells (24), and knockdown of Tβ4 attenuated sphere-forming capacities in vitro and tumorigenicity in vivo by promoting differentiation in glioma cells (25). Thus, Tβ4 could cause gain of cancer stem cell-like phenotypes, consistent with the present data.

Epigenetic alterations have increasingly been recognized as integral for their possible roles in treatment resistance (11). However, all the anti-cancer drugs used in these studies target cancer cells, not tumor microenvironment pathways such as angiogenesis, and are administered to cancer cells for the generation of resistant subclones in vitro, not in vivo (12-15). In contrast, we have identified that H3K4me3 and H3K27ac levels were globally elevated in the HCC cells surviving under the inhibition of angiogenesis, providing the first evidence that dynamic epigenetic states of cancer cells could be influenced by modulating the tumor microenvironment in vivo. In this work, we particularly focused on epigenetic regulation of Tβ4, and observed that the Tβ4 promoter region in the drug-resistant HuH7 cells was demethylated and enriched with active histone marks H3K4me3 and H3K27ac, that is, exhibited open chromatin states. Cumulative findings indicate that an open chromatin state contributes to maintenance of pluripotency in stem cells and also dedifferentiation with aberrant activation of oncogenes in cancer cells (26), and then were consistent with the current

observation of the similar epigenetic alterations during acquisition of stemness and drug resistance in this study. Knoechel et al. have recently discovered that a chromatin regulator BRD4 binds acetylated histones linked with open chromatin structures at the enhancers of critical genes like *MYC* and *BCL2* to facilitate the gene transcription in the drug-tolerant persisters of T cell acute lymphoblastic leukemia (14). They have also reported the intriguing data that a BRD4 inhibitor JQ1 triggered growth arrest and apoptosis specifically in the resistant cells by decreasing core gene expression, which implies that epigenetic drugs antagonizing chromatin regulators recruited at the Tβ4 promoter locus can sensitize the resistant HCC cells to anti-angiogenic therapy (14).

In summary, we here established a xenograft model of anti-angiogenic therapy resistance by long-term exposure with serial transplantation, which closely mimics clinical conditions. This process was accompanied with the gain of cancer stem cell-like features and epigenetic alterations inducing the aberrant expression of Tβ4. Tβ4 was responsible for the drug resistance, and then could be the molecular target as well as the surrogate marker for sorafenib antiangiogenic treatment in patients with advanced HCC.

**Acknowledgments**

We thank Ms. Hiromi Nagasaki for technical assistance.

## References

1. Ferlay J, Soerjomataram I, Dikshit R, Eser S, Mathers C, Rebelo M, *et al.* Cancer incidence and mortality worldwide: sources, methods and major patterns in GLOBOCAN 2012. *Int J Cancer* **2015**;136:E359-86.
2. Marquardt JU, Andersen JB, Thorgeirsson SS. Functional and genetic deconstruction of the cellular origin in liver cancer. *Nat Rev Cancer* **2015**;15:653-67.
3. Llovet JM, Villanueva A, Lachenmayer A, Finn RS. Advances in targeted therapies for hepatocellular carcinoma in the genomic era. *Nat Rev Clin Oncol* **2015**;12:436.
4. Zhu AX. New agents on the horizon in hepatocellular carcinoma. *Ther Adv Med Oncol* **2013**;5:41-50.
5. Bruix J, *et al.* Regorafenib for patients with hepatocellular carcinoma who progressed on sorafenib treatment (RESORCE): a randomised, double-blind, placebo-controlled, phase 3 trial. *Lancet* **2016**; doi: 10.1016/S0140-6736(16)32453-9.
6. Nakao K, Tanaka S, Miura T, Sato K, Matsumura S, Aihara A, *et al.* Novel Aurora/vascular endothelial growth factor receptor dual kinase inhibitor as treatment for hepatocellular carcinoma. *Cancer Sci* **2015**;106:1016-22.

7. Bergers G, Hanahan D. Modes of resistance to anti-angiogenic therapy. *Nat Rev Cancer* **2008**;8:592-603.

8. Allegra CJ, Yothers G, O'Connell MJ, Sharif S, Petrelli NJ, Colangelo LH, *et al.* Phase III trial assessing bevacizumab in stages II and III carcinoma of the colon: results of NSABP protocol C-08. *J Clin Oncol* **2011**;29:11-6.

9. Pàez-Ribes M, Allen E, Hudock J, Takeda T, Okuyama H, Viñals F, *et al.* Antiangiogenic therapy elicits malignant progression of tumors to increased local invasion and distant metastasis. *Cancer Cell* **2009**;15:220-31.

10. Thorgeirsson SS. Stemness and reprogramming in liver cancer. *Hepatology* **2016**;63:1068-70.

11. Easwaran H, Tsai HC, Baylin SB. Cancer epigenetics: tumor heterogeneity, plasticity of stem-like states, and drug resistance. *Mol Cell* **2014**;54:716-27.

12. Fan M, Yan PS, Hartman-Frey C, Chen L, Paik H, Oyer SL, *et al.* Diverse gene expression and DNA methylation profiles correlate with differential adaptation of breast cancer cells to the antiestrogens tamoxifen and fulvestrant. *Cancer Res* **2006**;66:11954-66.

13. Sharma SV, Lee DY, Li B, Quinlan MP, Takahashi F, Maheswaran S, *et al.* A chromatin-mediated reversible drug-tolerant state in cancer cell subpopulations. *Cell* **2010**;141:69-80.

14. Knoechel B, Roderick JE, Williamson KE, Zhu J, Lohr JG, Cotton MJ, *et al.* An epigenetic mechanism of resistance to targeted therapy in T cell acute lymphoblastic leukemia. *Nat Genet* **2014**;46:364-70.

15. Ito H, Tanaka S, Akiyama Y, Shimada S, Adikrisna R, Matsumura S, *et al.* Dominant Expression of DCLK1 in Human Pancreatic Cancer Stem Cells Accelerates Tumor Invasion and Metastasis. *PLoS One* **2016**;11:e0146564.

16. Teicher BA, Herman TS, Holden SA, Wang YY, Pfeffer MR, Crawford JW, *et al.* Tumor resistance to alkylating agents conferred by mechanisms operative only in vivo. *Science* **1990**;247:1457-61.

17. Ramalho-Santos M, Yoon S, Matsuzaki Y, Mulligan RC, Melton DA. "Stemness": transcriptional profiling of embryonic and adult stem cells. *Science* **2002**;298:597-600.

18. Cairo S, Armengol C, De Reyniès A, Wei Y, Thomas E, Renard CA, *et al.* Hepatic stem-like phenotype and interplay of Wnt/beta-catenin and Myc signaling in aggressive childhood liver cancer. *Cancer Cell* **2008**;14:471-84.

19. Hoshida Y, Nijman SM, Kobayashi M, Chan JA, Brunet JP, Chiang DY, *et al.* Integrative transcriptome analysis reveals common molecular subclasses of human hepatocellular carcinoma. *Cancer Res* **2009**;69:7385-92.

20. Boyault S, Rickman DS, de Reyniès A, Balabaud C, Rebouissou S, Jeannot E, *et al.* Transcriptome classification of HCC is related to gene alterations and to new therapeutic targets. *Hepatology* **2007**;45:42-52.

21. Tovar V, Cornella H, Moeini A, Vidal S, Hoshida Y, Sia D, *et al.* Tumour initiating cells and IGF/FGF signalling contribute to sorafenib resistance in hepatocellular carcinoma. *Gut* **2015**;doi: 10.1136/gutjnl-2015-309501.

22. Sato K, Tanaka S, Mitsunori Y, Mogushi K, Yasen M, Aihara A, *et al.* Contrast-enhanced intraoperative ultrasonography for vascular imaging of hepatocellular carcinoma: clinical and biological significance. *Hepatology* **2013**;57:1436-47.

23. Rudalska R, Dauch D, Longerich T, McJunkin K, Wuestefeld T, Kang TW, *et al.* In vivo RNAi screening identifies a mechanism of sorafenib resistance in liver cancer. *Nat Med* **2014**;20:1138-46.

24. Wang WS, Chen PM, Hsiao HL, Wang HS, Liang WY, Su Y. Overexpression of the thymosin beta-4 gene is associated with increased invasion of SW480 colon

carcinoma cells and the distant metastasis of human colorectal carcinoma. *Oncogene* **2004**;23:6666-71.

25. Wirsching HG, Krishnan S, Florea AM, Frei K, Krayenbühl N, Hasenbach K, *et al.* Thymosin β 4 gene silencing decreases stemness and invasiveness in glioblastoma. *Brain* **2014**;137:433-48.

26. Gaspar-Maia A, Alajem A, Meshorer E, Ramalho-Santos M. Open chromatin in pluripotency and reprogramming. *Nat Rev Mol Cell Biol* **2011**;12:36-47.

## Figure Legends

**Figure 1**. Acquired resistance to anti-angiogenic therapy in HCC cells during long-term administration of VEGFR inhibitor. **A,** Schematic representation of the establishment of clonal HCC cells resistant to anti-angiogenic therapy in vivo. Human HCC cell line HuH7 was injected into NOD/SCID mice to generate subcutaneous tumors, and after treatment with VEGFR inhibitor JNJ-28841072, the remnant tumors were transplanted into the next group of mice. This process was repeatedly performed 12 times, and resistant subclones were established. **B,** Tumor reduction ratio of HuH7-F0 (parental) and -F12 (drug-resistant) cells in the NOD/SCID mice treated with JNJ-28841072. Bars are the mean ± SD. *, $P < 0.001$ by Student's $t$ test. **C,** Kaplan-Meier curves of the overall survival in the NOD/SCID mice with the treatment of sorafenib (30 mg/kg/day). Blue, purple, and orange lines represent HuH7-F0, -F6 and -F12, and solid and dotted lines represent samples treated and untreated with sorafenib, respectively ($n = 10$). *, $P < 0.001$, †not significant by the log-rank test. **D,** Tumor reduction ratio of HuH7-F0, -F6 and -F12 cells in the NOD/SCID mice treated with sorafenib. Bars are the mean ± SD. *, $P < 0.001$ by ANOVA with Dunnett's post hoc test.

**Figure 2.** Comparative analysis of gene expression between the drug-resistant and

-sensitive HCC cells. **A,** Enrichment plots of gene sets associated with the HuH7 cells resistant to anti-angiogenic therapy. The upper two gene sets are enriched in stem cell-like population (17) and hepatoblastoma (18), and the lower two are composed of genes upregulated in S2 subtype of Hoshida's classification (19) and G3 subtype of Boyault's classification (20), respectively. NES, normalized enrichment score. FDR, false discovery rate. **B,** Venn diagram of genes more than four-fold upregulated in HuH7-F6 and -F12 compared with HuH-F0. **C,** Relative expression levels of Tβ4 and CD133 in HuH7-F0, -F6 and -F12 cells at the mRNA level. Bars are the mean ± SD. *, $P < 0.001$ by ANOVA with Dunnett's post hoc test.

**Figure 3.** Methylation status at the Tβ4 promoter in the HuH7 sublines. **A,** RT-PCR analysis of Tβ4 in HuH7 cells treated with epigenetic drugs. Cells were exposed to 100 nM 5-aza-2'-deoxycytidine (5-aza) for 72 hours or 300 nM trichostatin A (TSA) for 48 hours. **B,** Schematic representation of the genomic structure and CpG island predicted by the MethPrimer program of the *TMSB4X* gene, encoding Tβ4. Boxes denote the exons of Tβ4. Individual CpG sites are shown as vertical lines. The upper and lower double-headed arrows indicate the regions examined by bisulfite sequencing (BSS) and methylation-specific PCR (MSP), respectively. **C,** MSP analysis of Tβ4 in HuH7-F0,

-F6 and -F12 cells. U and M denote the PCR products with unmethylation and methylation-specific primers, respectively. **D,** BSS analysis of Tβ4. Open and closed squares indicate unmethylated and methylated CpG sites, respectively. A double-headed arrow show the region analyzed by MSP. Methylation levels are calculated as the proportion of methylated to total cytidine at the CpG sites.

**Figure 4.** Histone modification status at the Tβ4 promoter and at the protein level in the HuH7 sublines. **A,** Schematic representation of the genomic structure of the *Tβ4* gene for ChIP assay. Boxes denote the exons of Tβ4. The three double-headed arrows indicate the regions examined by ChIP assay. **B,** Histone modification status in HuH7-F0 and -F12 cells. ChIP assay was conducted by using antibodies against active (H3K4me3 and H3K27ac) and repressive (H3K9me3 and H3K27me3) histone remarks at the three regions CP1, CP2 and CP3. Representative images and semi-quantification measurements are displayed. **C,** Quantitative ChIP analysis of Tβ4 at the region CP2 in HuH7-F0, -F6 and -F12 cells. Bars are the mean ± SE. *, $P < 0.01$ by ANOVA with Dunnett's post hoc test. **D,** Immunoblots of H3K4me3 and H3K27ac.

**Figure 5.** Biological effects of Tβ4 on the cancer cells in vitro. **A,** Immunofluorescence

analysis of HuH7-F0, -F12 and -Tβ4 with Tβ4 staining (red). Nuclei were counterstained with DAPI (blue). Magnification, ×200. **B,** Quantification of sphere-forming efficiency. Bars are the mean ± SD. *, $P < 0.001$ by ANOVA with Dunnett's post hoc test. **C,** Transwell migration assay. **D,** Matrigel invasion assay. The number of motile and infiltrating cells was estimated and is displayed in the upper panels. Bars are the mean ± SD. *, $P < 0.01$ by ANOVA with Dunnett's post hoc test. Representative images are shown in the lower panels. Magnification, ×200.

**Figure 6.** Biological effects of Tβ4 on the cancer cells in vivo. **A,** Tumor-growth curves of HuH7-F0, -F12 and -Tβ4 cells. Bars are the mean ± SE. *, $P < 0.05$ by ANOVA with Dunnett's post hoc test. **B,** Immunohistochemical analysis of Tβ4 expression in the transplanted tumors of each group. Nuclei were counterstained with hematoxylin. Serial sections of the samples were stained with hematoxylin and eosin (HE). Magnification, ×200. C**,** Kaplan-Meier curves of the overall survival in the NOD/SCID mice subcutaneously transplanted with HuH7-F0, -F12 and -Tβ4 cells under the oral administration of sorafenib (30 mg/kg/day). Blue, orange, and green lines represent HuH7-F0, -F12 and -Tβ4, and solid and dotted lines represent samples treated and untreated with sorafenib, respectively ($n = 10$). *, $P < 0.001$, †not significant by the

log-rank test. **D,** Tumor reduction ratio of each cell line in the NOD/SCID mice with sorafenib treatment. *, $P < 0.001$ by ANOVA with Dunnett's post hoc test. **E,** Immunohistochemical analysis of CD31 endothelial marker in the transplanted tumors of each group with or without sorafenib treatment. Nuclei were counterstained with hematoxylin. Magnification, ×200. **F,** Reduction ratio of tumor vessel area with CD31 expression. *, $P < 0.01$, †, not significant by the Kruskal-Wallis test with Steel-Dwass multiple comparisons test.

**Figure 7.** Correlation between Tβ4 expression in primary HCC and prognosis of the patients. **A,** Immunohistochemical analysis of tissue samples for Tβ4-low and -high HCC in patients with sorafenib treatment. Nuclei were counterstained with hematoxylin. Serial sections of the samples were stained with HE. **B,** Kaplan-Meier curves of the progression-free survival in sorafenib-treated patients with Tβ4-low ($n = 23$) and -high HCC ($n = 7$). The *P*-value was calculated by the log-rank test.

**Figure 1** Author Manuscript Published OnlineFirst on February 28, 2017; DOI: 10.1158/1535-7163.MCT-16-0728
Author manuscripts have been peer reviewed and accepted for publication but have not yet been edited.

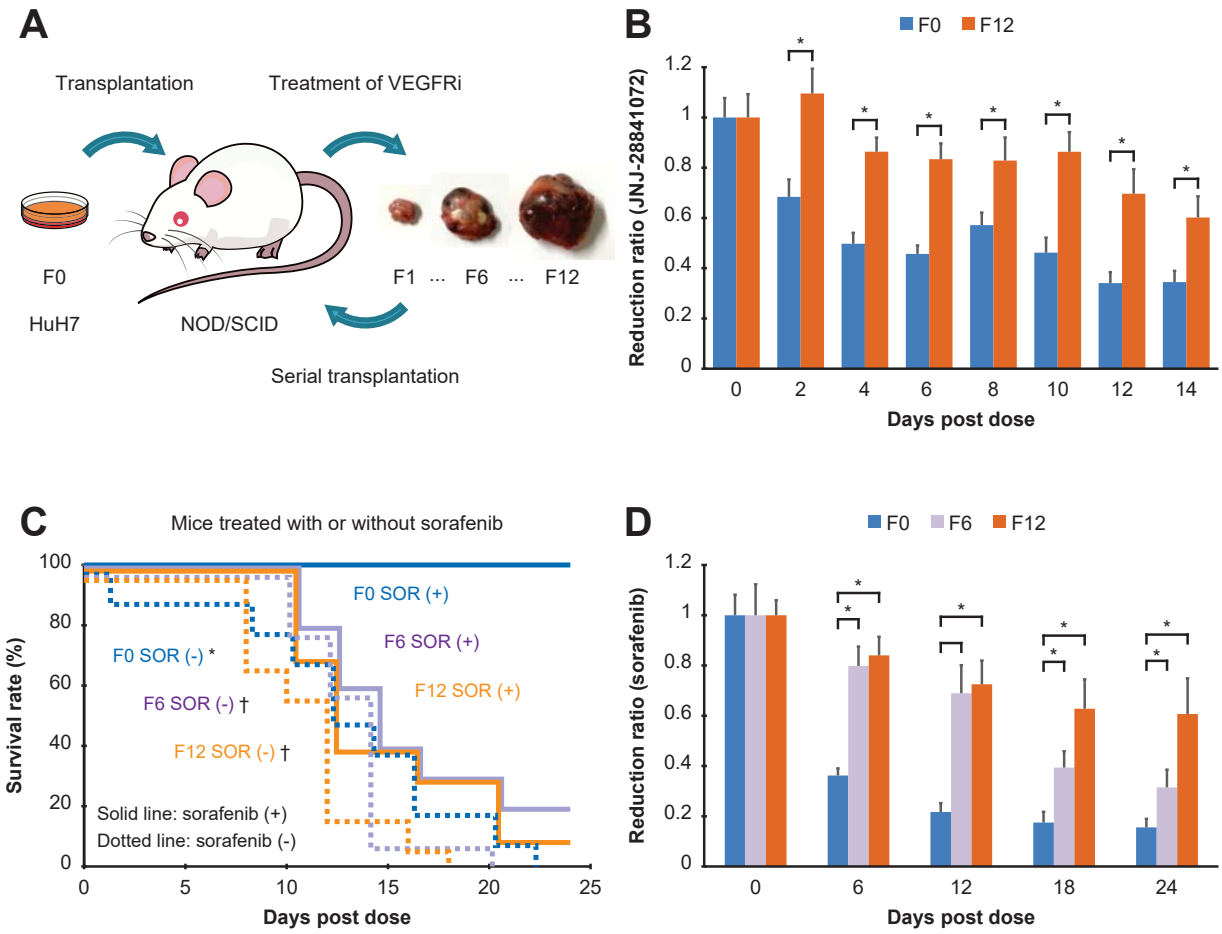

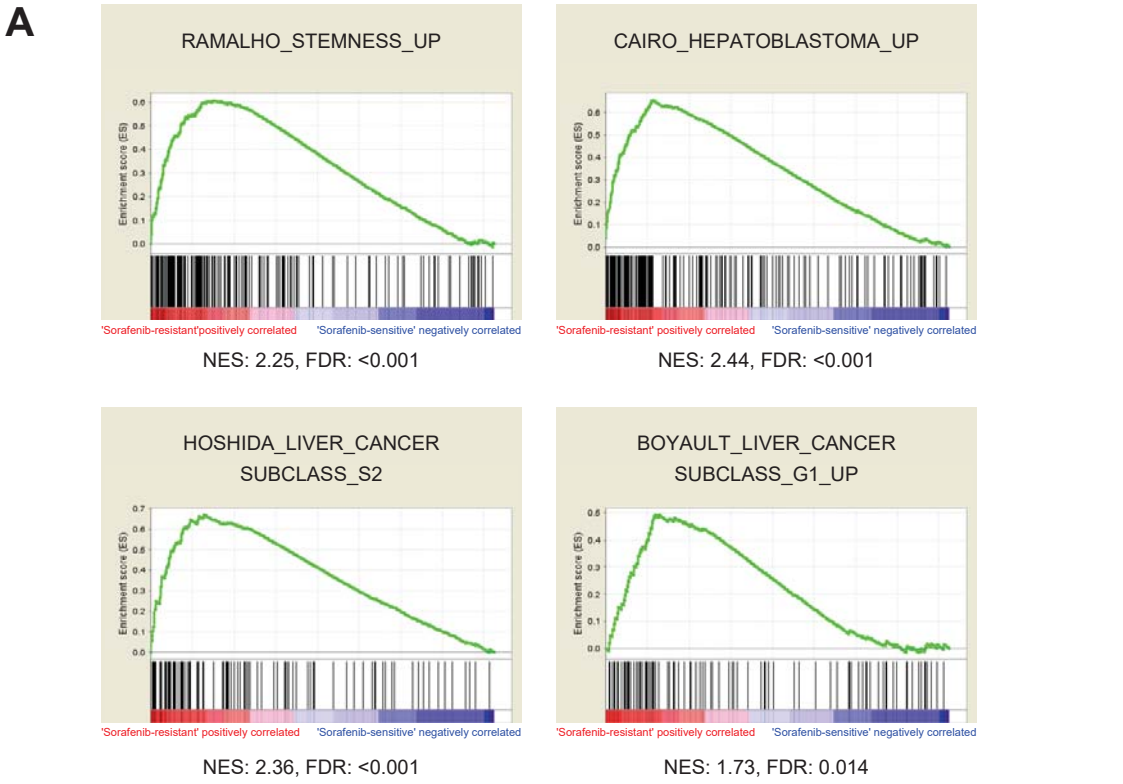


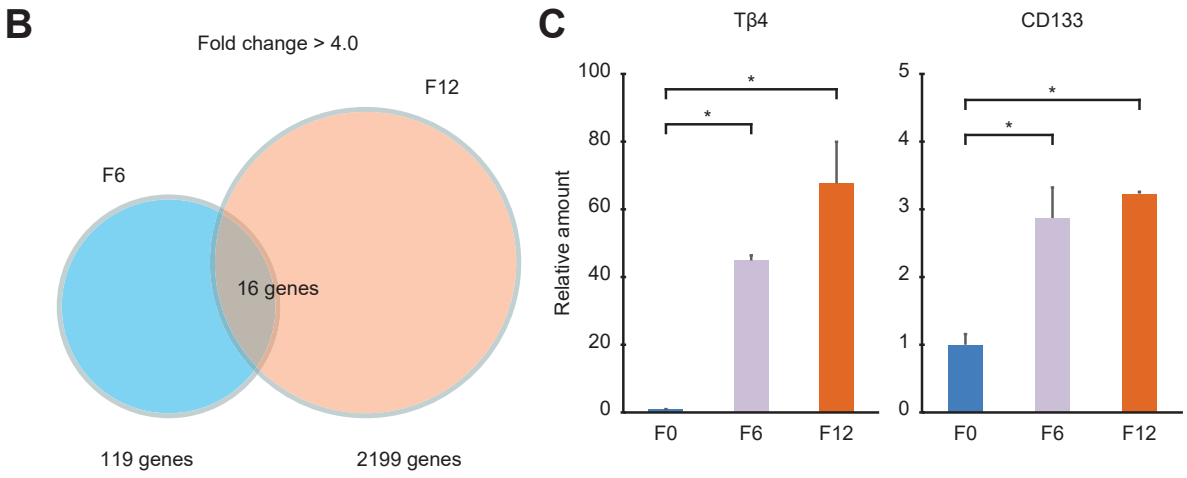

Author Manuscript Published OnlineFirst on February 28, 2017; DOI: 10.1158/1535-7163.MCT-16-0728


**Figure 3**

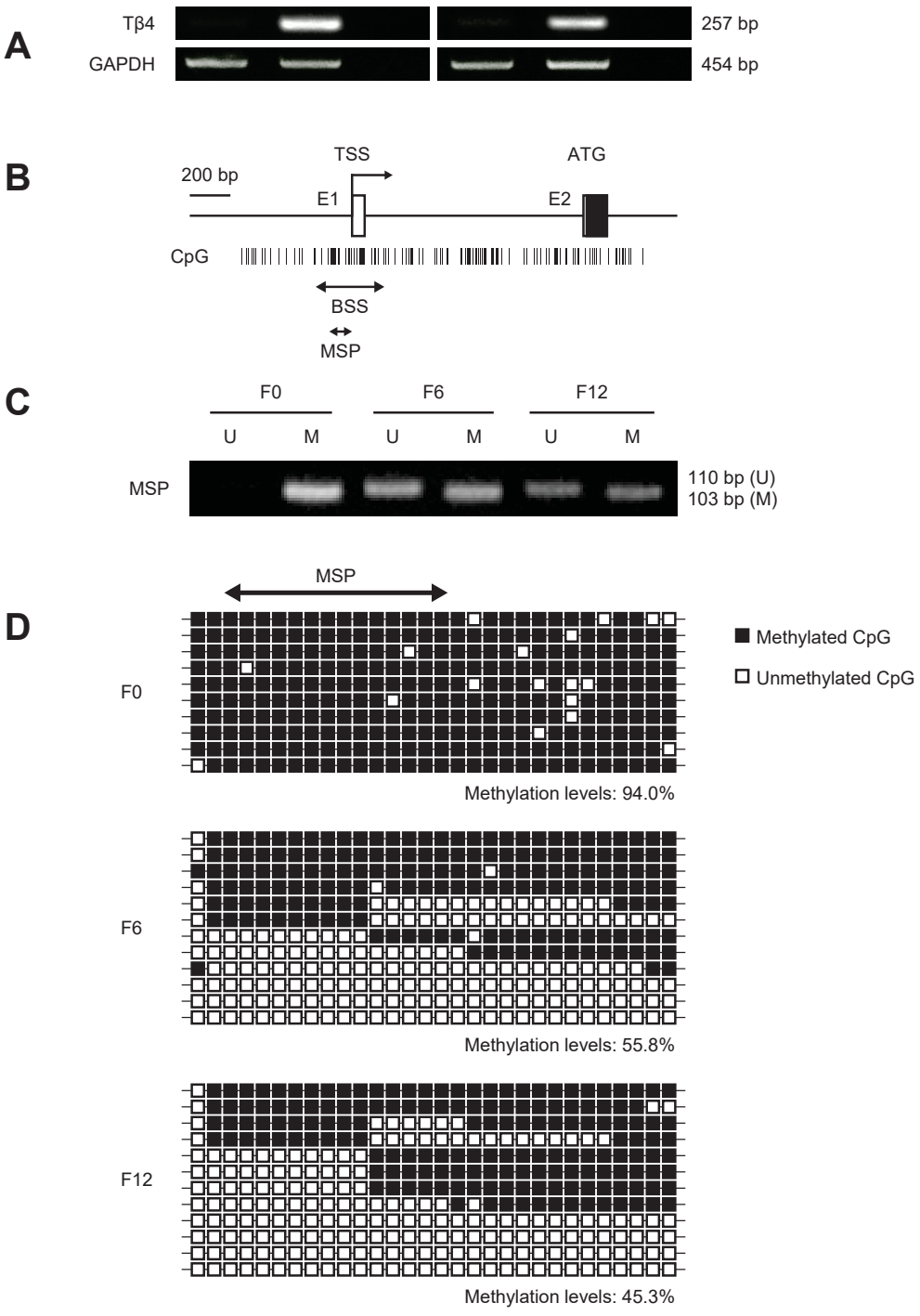

Author Manuscript Published OnlineFirst on February 28, 2017; DOI: 10.1158/1535-7163.MCT-16-0728
Author manuscripts have been peer reviewed and accepted for publication but have not yet been edited.

**Figure 4**

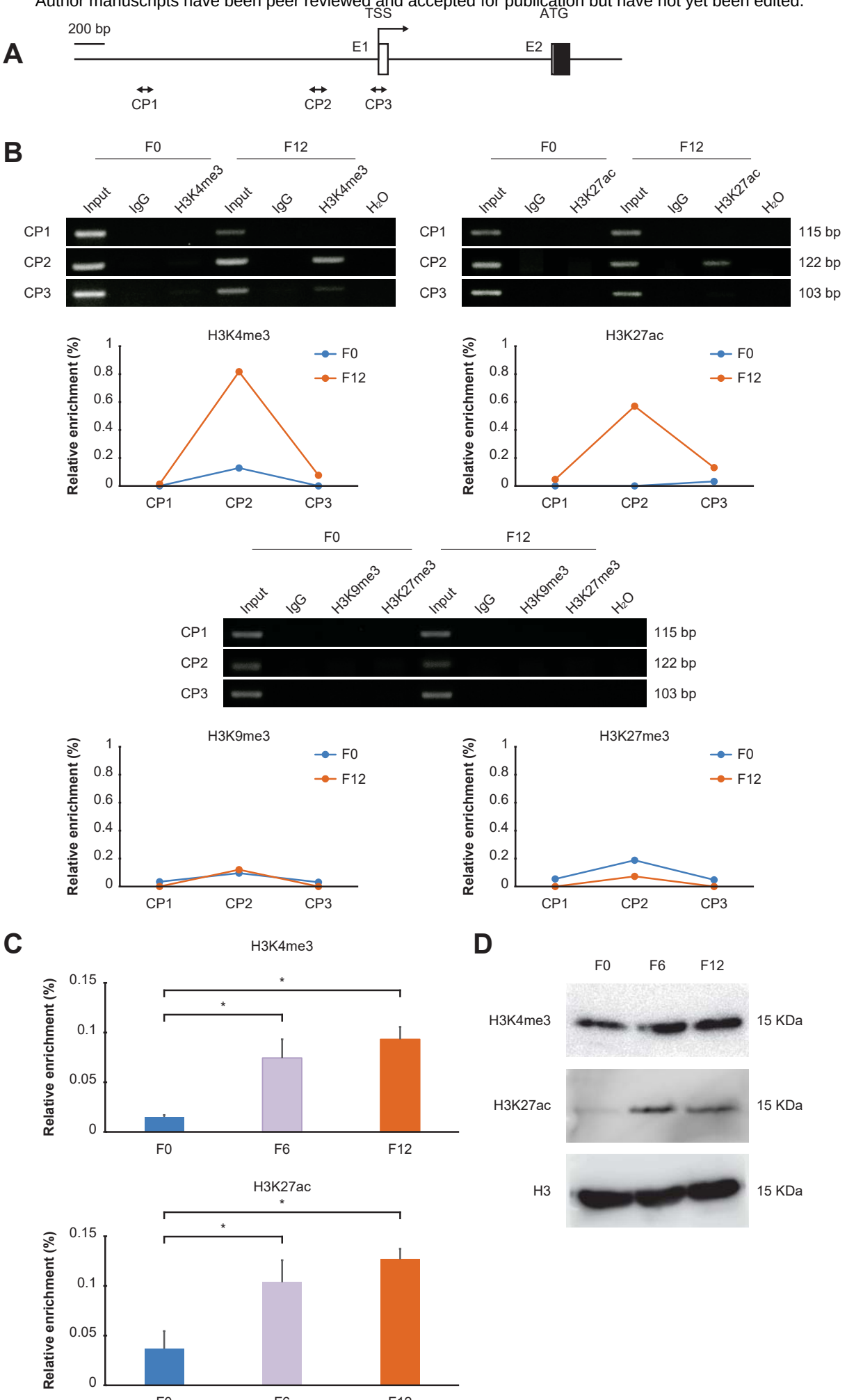

Author Manuscript Published OnlineFirst on February 28, 2017; DOI: 10.1158/1535-7163.MCT-16-0728
Author manuscripts have been peer reviewed and accepted for publication but have not yet been edited.

**Figure 5**

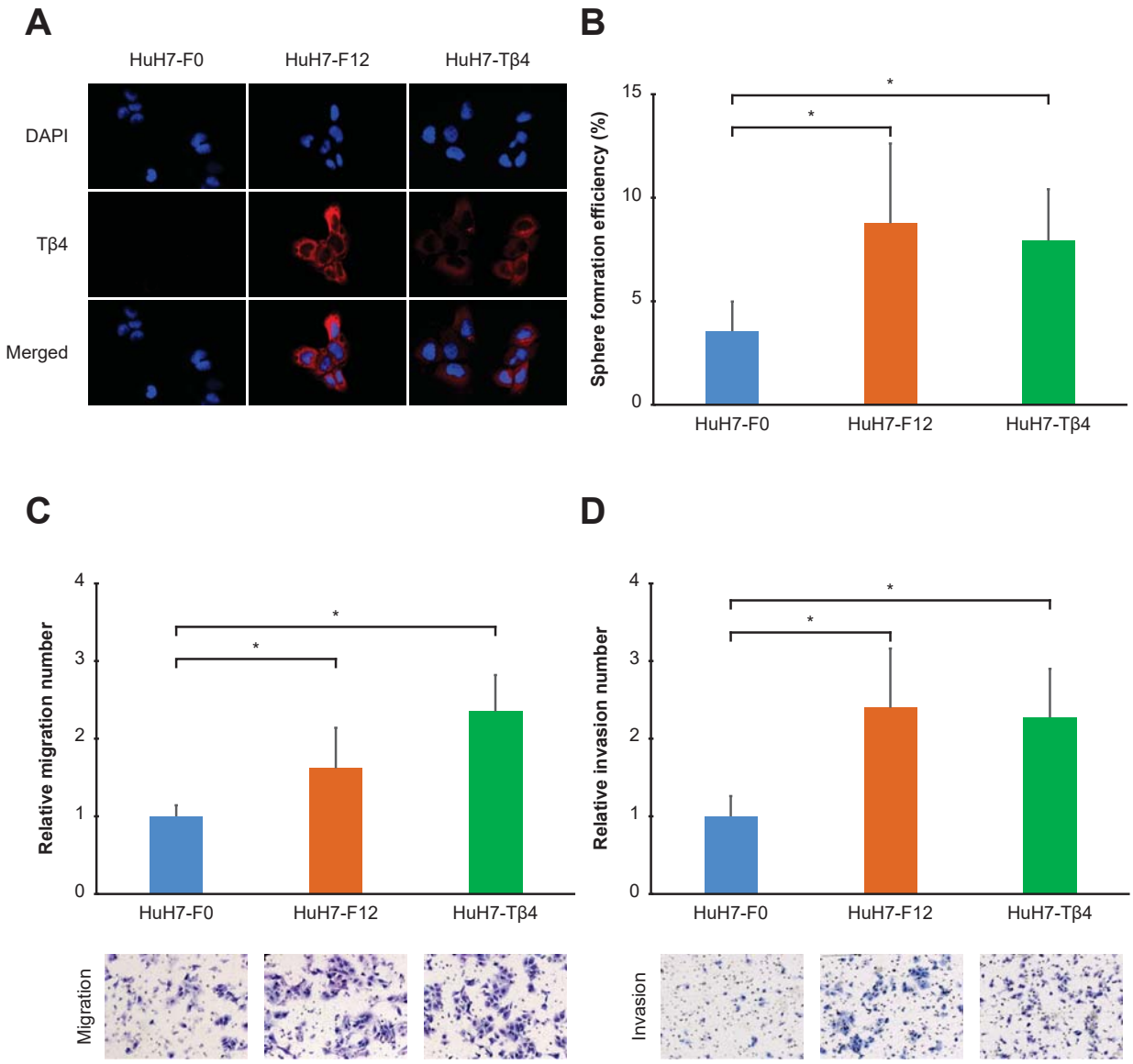

Author Manuscript Published OnlineFirst on February 28, 2017; DOI: 10.1158/1535-7163.MCT-16-0728
Author manuscripts have been peer reviewed and accepted for publication but have not yet been edited.

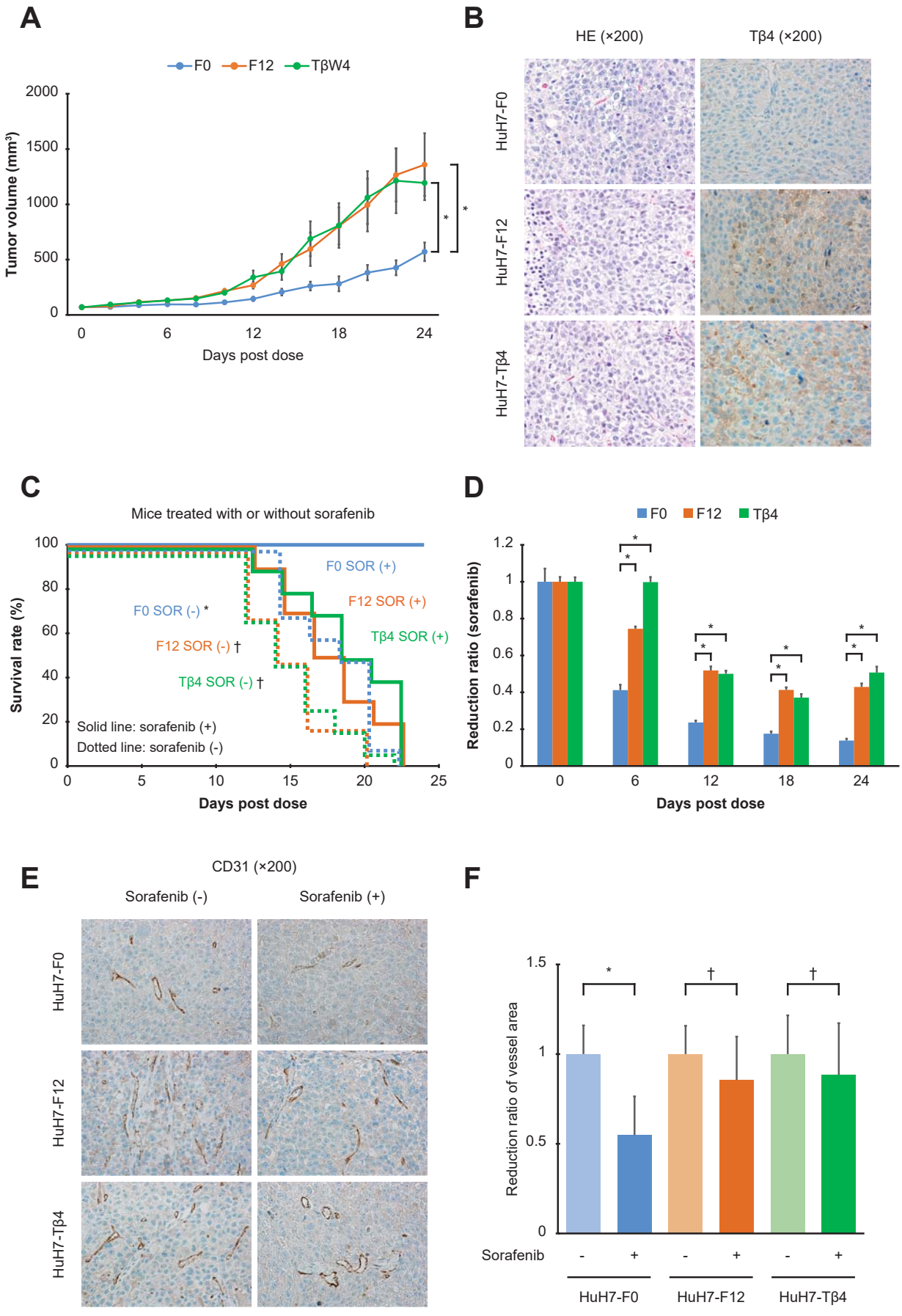

**Figure 7** Author Manuscript Published OnlineFirst on February 28, 2017; DOI: 10.1158/1535-7163.MCT-16-0728
Author manuscripts have been peer reviewed and accepted for publication but have not yet been edited.

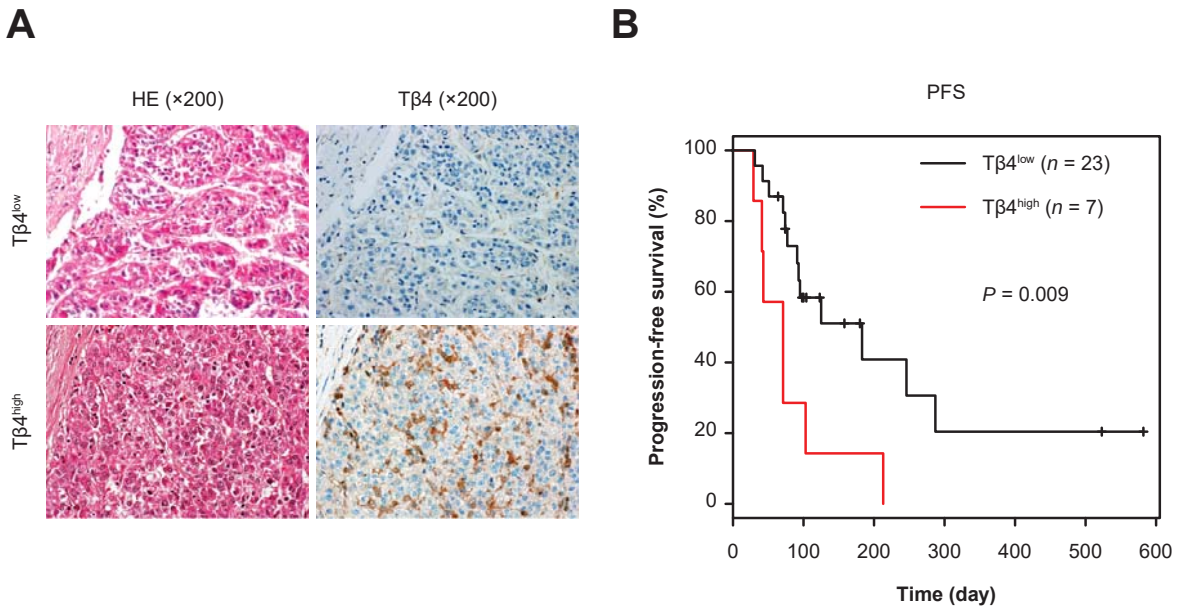

AACR American Association for Cancer Research

Molecular Cancer Therapeutics

# Acquired resistance with epigenetic alterations under long-term anti-angiogenic therapy for hepatocellular carcinoma

Yoshiteru Ohata, Shu Shimada, Yoshimitsu Akiyama, et al.

*Mol Cancer Ther* Published OnlineFirst February 28, 2017.